METHODS OF DEPOSITING ANTI-REFLECTIVE COATINGS FOR ADDITIVELY MANUFACTURED OPTICS

Z. J. Beller*, E. B. Secor*, J. Lavin*, D. M. Keicher†, M. Essien†, S. Whetten*, S. S. Mani*

*Sandia National Laboratories
†Integrated Deposition Solutions, Inc.

Abstract

Recent advancements in the field of additive manufacturing (AM) have enabled the production of high-fidelity optical components allowing for the design of novel fiber optic systems. In order to support this emerging technology, methods of depositing anti-reflective coatings (ARCs) onto these optical components must be developed. Work has begun to identify such coating materials; develop systems capable of accurately depositing controlled, uniform layers onto given substrates; establish deposition procedures for ensuring coating validity; and establish post-processing procedures to ensure the reliability of finished components. Areas of interest for finished components include their integration into high-bandwidth fiber optic systems, enabling further miniaturization of communication components. Methods of ARC deposition will be discussed along with final component performance and the identification of key process parameters affecting product performance.

Introduction

The use of fiber optic connections and components to transmit information signals via light allows the bandwidth and rate of communication of a system to be greatly increased compared to traditional wired connections. However, system complexity and material constraints can restrict the development of such optical systems. Novel additive manufacturing (AM) techniques offer a promising means to implement these fiber optic components in a versatile platform [1]. Through these techniques, optical connections can be deposited directly into complex systems, where traditional manufacturing methods would require changes to the existing system.

In order to facilitate the further design and development of novel fiber optic connections, methods of depositing anti-reflective coatings (ARCs) must be established. In traditional fiber optic systems, ARCs limit the loss of light at junctions due to either undesired feedback or emission into the environment [2,3]. These traditional systems typically utilize coatings of magnesium fluoride deposited by atomic layer deposition (ALD) [4,5]. In ALD, the coating precursors are deposited alternately from the gas phase with self-terminating reactions to form thin, uniform layers. However, ALD typically produces a conformal coating without spatial selectivity, and would expose the entire system assembly to the coating rather than only the connectors. To limit this system-wide exposure to the coating material, a more targeted, conformal process of deposition must be established.

High performing ARCs must meet a strict geometric profile. Primarily, the film thickness and refractive index must satisfy the following conditions to optimally prevent the reflection of a given wavelength of light:

$$n_{ARC} = \sqrt{n_{env} * n_s} \tag{1}$$

$$d_{ARC} = \frac{k * \lambda}{4 * n_{ARC}} \tag{2}$$

in which n_{ARC}, n_{env}, and n_s are the indices of refraction for the film, environment, and substrate, respectively, d_{ARC} is the thickness of the ARC film, λ is the wavelength of light of interest, and k=1, 3, 5, etc [3]. Therefore, it is critical to the overall performance of the film that the thickness is as close to the calculated value as possible.

Experimental

A. Equipment

To establish a process for depositing controlled layers of aerosolized coating material onto a substrate, it was necessary to either identify or establish a technology capable of depositing materials with high spatial resolution while mitigating flow out of the intended deposition area and overspray onto the substrate. Additionally, due to the critical nature of final film geometry, such a process would also need to deposit materials into layers with precise thickness control. Based on these demands, an IDS NanoJet (NJ) system was utilized for this investigation (Figures 1-2), as it has been demonstrated to produce films from low viscosity inks with a thickness resolution as fine as 50 nm [6].
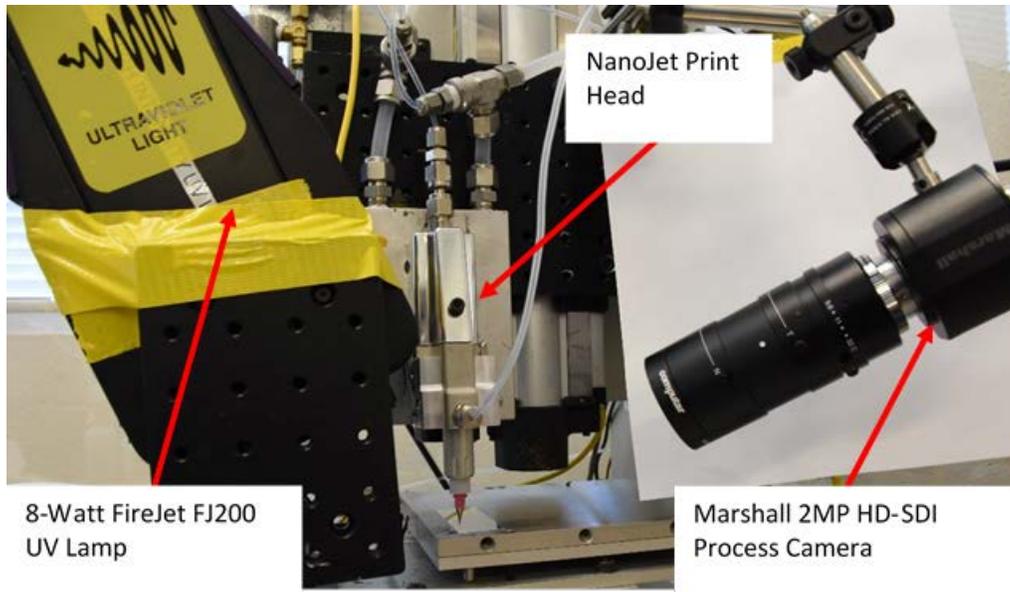
Figure 1. Photograph of the NanoJet system used in this study. The system features a Marshall compact 2MP HD-SDI camera for process monitoring, an 8-Watt FireJet FJ200 UV lamp for soft curing of the material, and the printhead to house, aerosolize, and deposit the materials of interest.
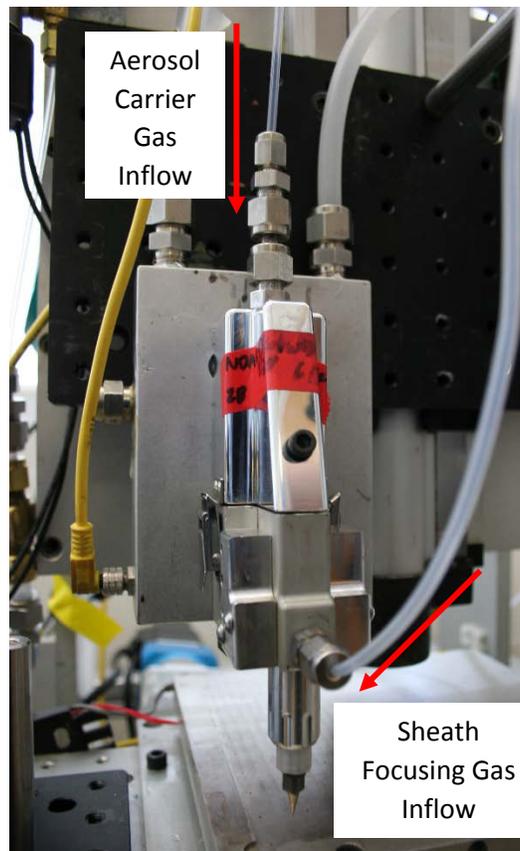
Figure 2. Close-up photograph of printhead. Inflows for both the aerosol carrier gas and sheath focusing gas are designated on the image.

In the NanoJet process, a liquid ink is aerosolized with an ultrasonic atomizer within the printhead. The aerosolized material is then transported via a carrier gas to the main flow channel of the printhead. In this main flow channel, an annular focusing gas is introduced to accelerate and collimate the aerosol stream. Due to the importance of the two gas flows and their control over the rate at which the aerosolized material is deposited, either flow rate can be altered to adjust the rate at which material is deposited.

B. Materials
The primary ink used to generate these coatings was a solution of isobutyl acetate and a commercially available UV curable optical adhesive (Norland Optical Adhesive NOA 89), and the substrate was a silicon wafer. Two different inks were tested with varying concentrations, the first containing 14:1 by volume isobutyl acetate/NOA 89 and the second with a 20:1 ratio by volume. These specific mixing ratios were selected for two primary reasons, to reduce the viscosity of the base optical adhesive and therefore promote atomization, and to reduce the concentration of the optical adhesive to more accurately control the thickness of each deposited layer, as less of the film material would be deposited per pass of the tool head. The resultant improvement in thickness resolution would enable broader tunability of films for different wavelengths. In both inks, the volatile isobutyl acetate was believed to completely evaporate

from the solutions following atomization or very rapidly upon impacting the substrate, leaving only the optical adhesive.

C. Process Parameters

During the deposition process, a cross-hatched toolpath was used that alternated depositing the material along the x and y-axes in subsequent layers (Figure 3). Such cross-hatching was used to prevent unintended flow and grain development in the films across multiple layers. Additionally, the target thickness of each film was dictated by the wavelength of light for final applications, and this was adjusted by varying the total number of layers printed. This investigation focused on a wavelength of 850 nm, so only a single layer of film material was deposited.
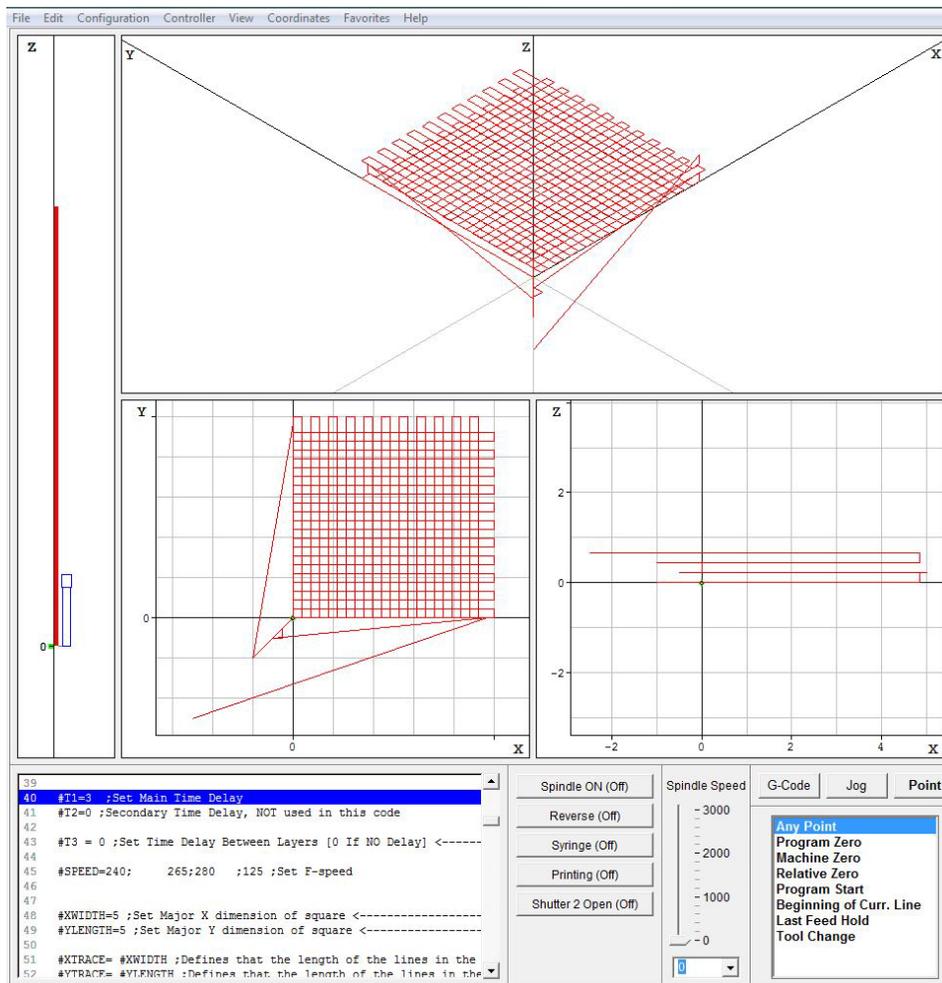
Figure 3. Screenshot of the toolpath generated to deposit the film material in a uniform geometry of controlled thickness.

Depending on the concentration of the material being deposited, several key process parameters were adjusted to facilitate film deposition, summarized in Table 1. For material mixed at a 14:1 concentration, compressed air was used for the aerosol carrier gas and the sheath focusing gas, with flow rates of 14.0 sccm and 11.0 sccm, respectively. The atomizer voltage was set to 41.5 V, and the substrate was heated to 60 °C. Additionally, the toolpath was run at a

feed rate, or print speed, of 220 mm/min, with an infill space between adjacent lines of 0.140 mm. Finally, throughout the deposition of the film, an 8-Watt FireJet FJ200 UV lamp was run at 10% power to soft cure the material as it was deposited. After each layer, the film was further cured for 180 seconds before the next layer was deposited.

For material mixed at a 20:1 concentration, the aerosol carrier gas and sheath focusing gas were set to flow rates of 12.0 sccm and 10.0 sccm, respectively. The atomizer voltage was set to 45.0 V, and the substrate was heated to 60 °C. Additionally, a feedrate of 180 mm/min was used, with an infill space between adjacent lines of 0.200 mm. Finally, throughout the deposition of the film, an 8-Watt FireJet FJ200 UV lamp was run at 30% power to soft cure the material as it was deposited. After each layer, the film was further cured for 180 seconds before the next layer was deposited.

Isobutyl Acetate:NOA 89 Concentration	14:1	20:1
Print Speed (mm/min)	220	180
Infill Spacing (mm)	0.140	0.200
Aerosol Flow Rate (sccm)	14.0	12.0
Sheath Flow Rate (sccm)	11.0	10.0
Atomizer Voltage (V)	41.5	45.0
Substrate Temperature (°C)	60	60
UV Lamp Output (% output)	10	30
Time Delay Between Layers (sec)	180	180

Table 1. Process parameters used to deposit each material mixture in the investigation. Only the print speed and the infill spacing were varied depending on the material.

Once fully deposited, each film was subjected to a three-stage curing process to finalize the samples. First, the films were thermally cured at 60 °C for 10minutes, 80 °C for 15 minutes, 100 °C for 10 minutes, and 120 °C for 20 minutes. This thermal stepping was intended to gradually drive off any remaining isobutyl acetate in the films. Next, the samples were cured under an ABM, Inc. Exposure System at a wavelength of 400 nm, at 500 W for 30 minutes to achieve a full cure of the NOA 89. Finally, one last thermal cure was applied to the films at 120 °C for 30 minutes.

Results and Discussion
A. Film Morphology
After all test films were fully cured, the morphology of the films was characterized to assess uniformity and thickness. Optical images reveal severe nonuniformity and inconsistency for films prepared with the 14:1 ink, while the 20:1 ink appears to offer a benefit based on the initial visual inspection (Figures 4-5).

Figure 4. An image nine fully cured test films (5mm X 5mm) of the 14:1 concentration ink deposited on a silicon wafer substrate.
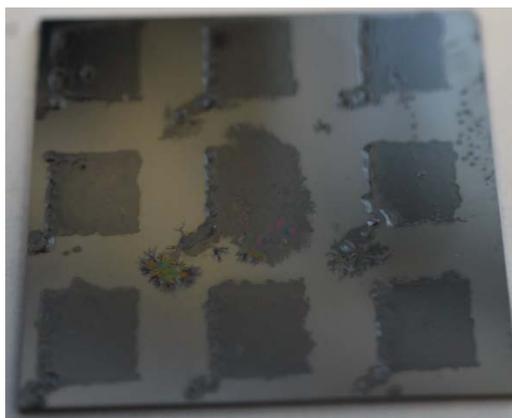
Figure 5. An image nine fully cured test films (5mm X 5mm) of the 20:1 concentration ink deposited on a silicon wafer substrate.

For more quantitative analysis, stylus profilometry was performed. For each film, 11 passes of profilometry were performed over the width of the sample. The first data corresponded to the ink containing a 14:1 mixture of isobutyl acetate and NOA 89. As expected from the optical image, the thicknesses of the films produced from the 14:1 material were extremely inconsistent. Across all nine films produced using the material, six films were wholly unusable do to issues in either the material beading up after deposition or simply not enough of the optical adhesive being deposited to produce a film of significant thickness. Despite these issues, three films were produced that roughly matched the intended geometry.

Profilometry of the three usable films shows an extreme lack of surface uniformity across the film areas (Figures 6-7). For these films, the average thickness ranged primarily between 0.5 µm and 1.5 µm; however, the variance in the average thickness of the films demonstrated an unpredictable thickness unsuitable for an optical component. Additionally, the film material built up around the perimeter of the films, suggesting that the material was still able to flow on the substrate after deposition despite the in-situ UV curing.
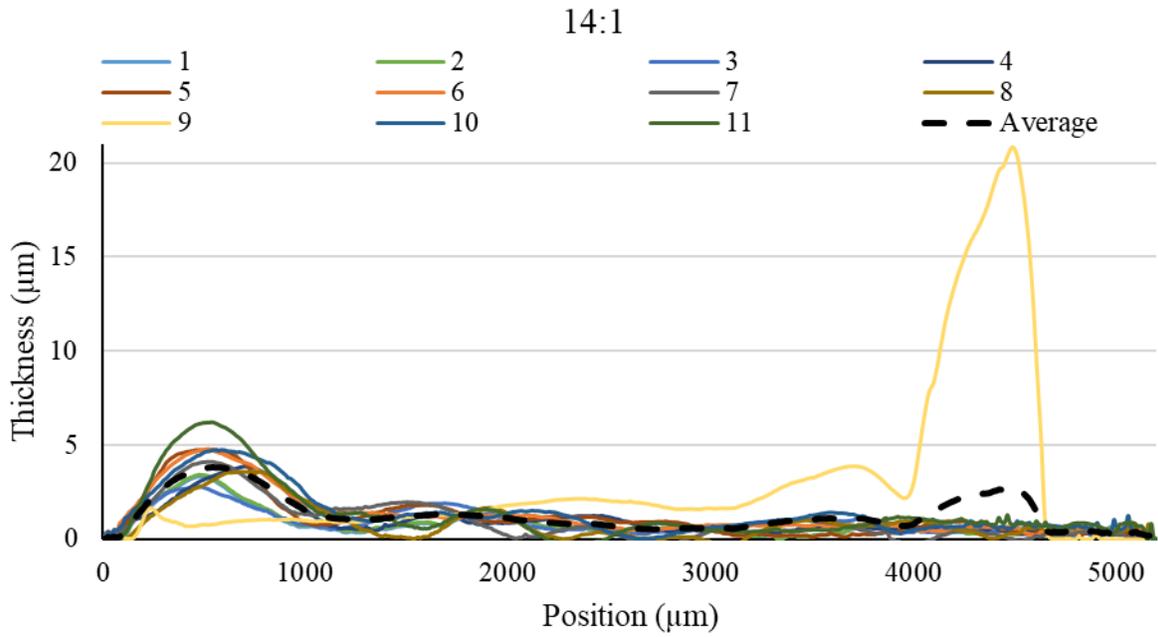
Figure 6. Plot of 11 measurements of thickness of a single film produced with the 14:1 material, as well as the average of the data sets.
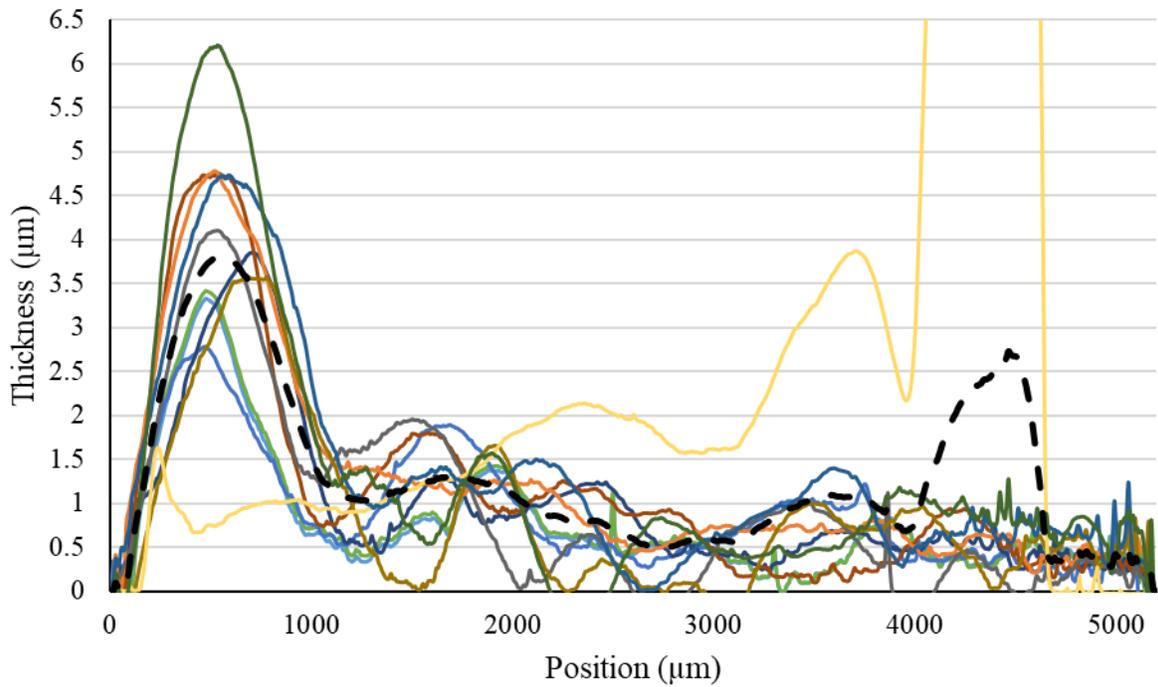
Figure 7. Plot of 11 measurements of thickness of a single film produced with the 14:1 material, as well as the average of the data sets. The Y-axis has been adjusted to offer a better view of the data.

Profilometry was also performed on the films produced from the ink with a 20:1 mixture of isobutyl acetate and NOA 89 (Figures 8-9). The films produced using this ink were much more consistent than the 14:1 films, as all nine films roughly matched the intended geometry. Profilometry also confirmed that these films were far more uniform, with the average thickness of the films typically ranging between 1.0 µm and 2.0 µm. Qualitatively, the measured thicknesses of the films never dramatically deviated from the average, demonstrating a promising uniformity in thickness that would not disqualify the films from being used in optical applications. Additionally, the film thickness steadily increased over the course of the film, showing that the material was not fully cured by the in-situ UV curing and instead flowed on the substrate. To mitigate this material flow, different printing and curing parameters should be explored for future film production.
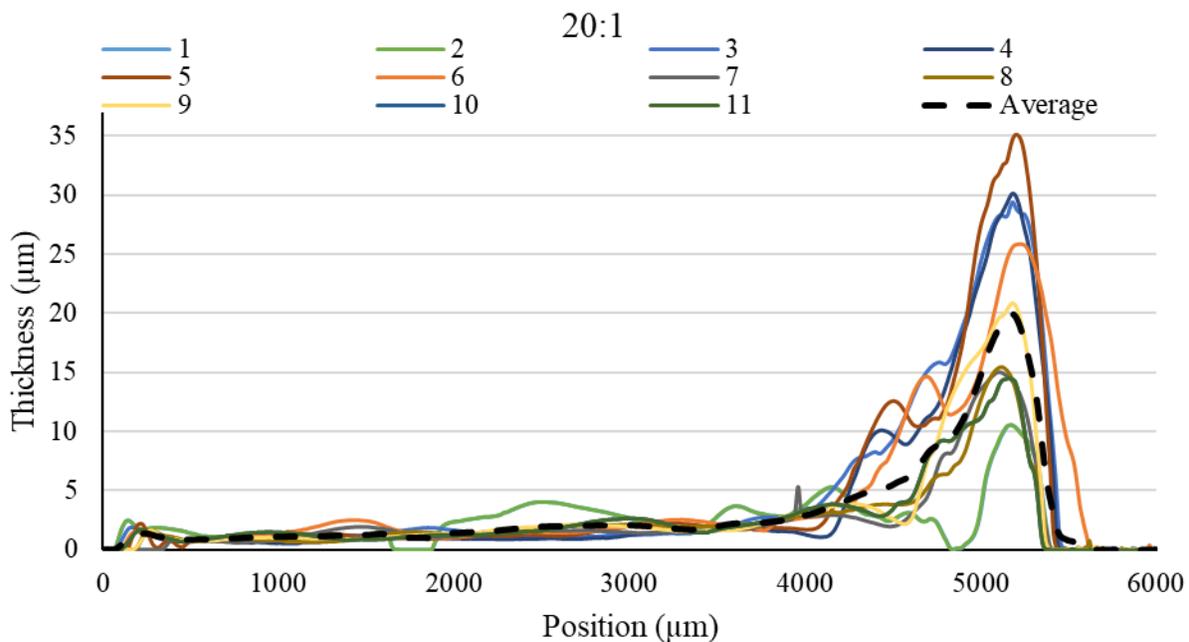
Figure 8. Plot of 11 measurements of thickness of a single film produced with the 20:1 material, as well as the average of the data sets.
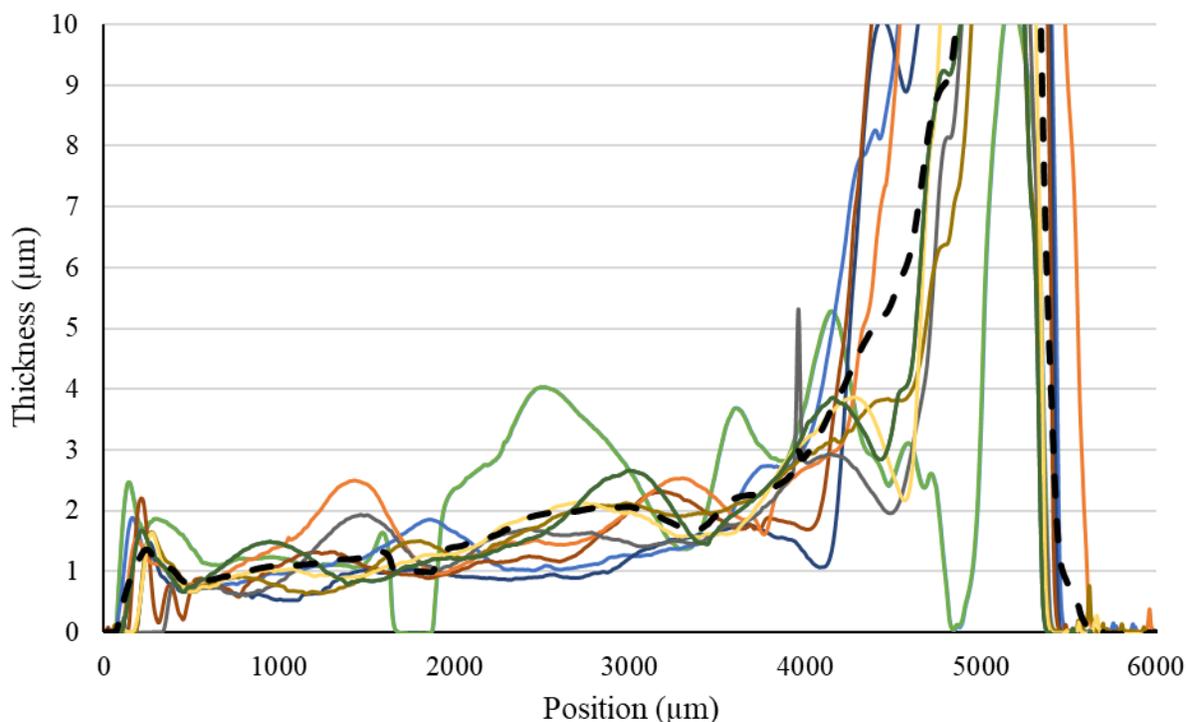
Figure 9. Plot of 11 measurements of thickness of a single film produced with the 20:1 material, as well as the average of the data sets. The Y-axis has been adjusted to offer a better view of the data.

B. Film Performance and Reflectivity of Near-Infrared Light

To gain an understanding of the optical properties of the printed films, spectroscopic ellipsometry was utilized to measure the reflectivity and optical thickness of sample lines of each material. In measuring the reflectivity of the films, special emphasis was given to the 850 nm wavelength, as this is a common operating condition of typical fiber-optic systems.

Due to the severe lack of surface uniformity in the sample films produced with the material mixed at a 14:1 ratio of isobutyl acetate to NOA 89, it was deemed that any data collected via spectroscopic ellipsometry would not be representative of the entire film. As such, it was decided that before any meaningful optical properties could be measured and recorded, future work needed to be conducted to improve the surface uniformity of films produced using this specific material composition.

The reflectivity of the material mixed at a 20:1 ratio of isobutyl acetate to NOA 89 was measured, and the value was recorded across a range of wavelengths. The response of the material across this spectrum can be seen in the Figures 10-11:
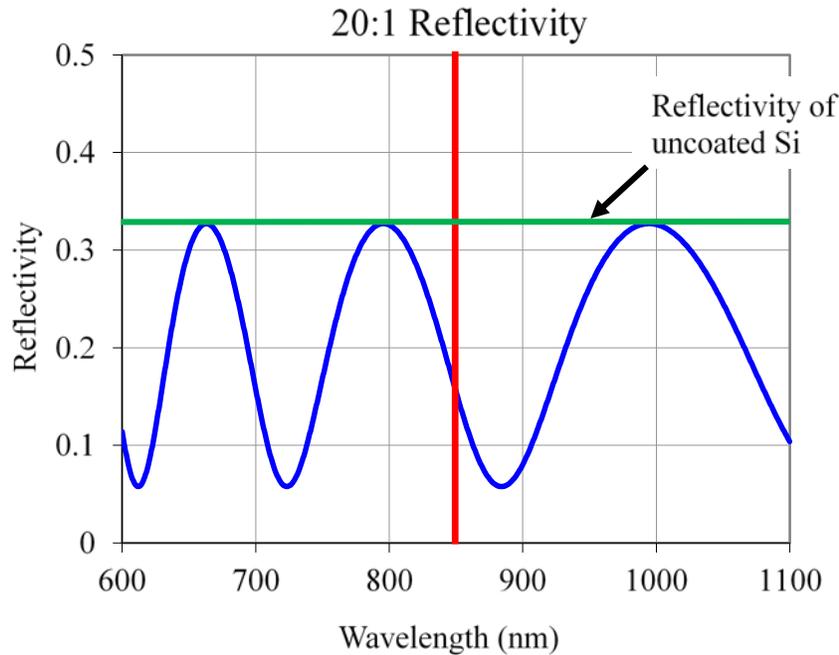
Figure 10. Reflectivity of the film produced with the 20:1 ink from 600-1100 nm. The green line represents the typical reflectivity of the uncoated Si substrate, which was approximately 33%. The red line represents the emphasized wavelength of 850 nm, at which the film had a reflectivity of approximately 17%.
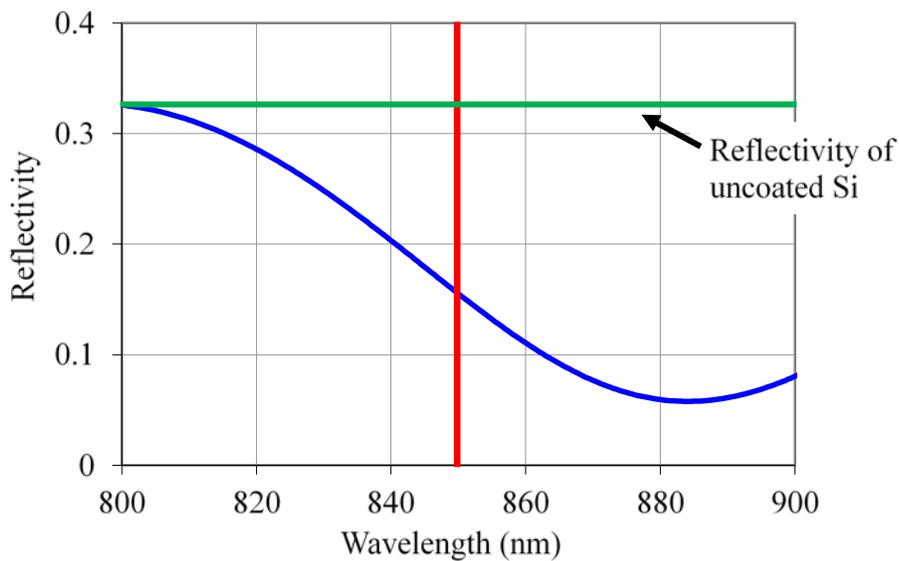
Figure 11. Reflectivity of the film printed with the 20:1 ink for wavelengths from 800-900 nm. The green line represents the typical reflectivity of the uncoated Si substrate, which was approximately 33%. The red line represents the emphasized wavelength of 850 nm, at which the film had a reflectivity of approximately 17%.

Prior to coating the Si wafer substrates with the isobutyl acetate/NOA 89 solution, the reflectivity of the uncoated substrate was measured and found to be approximately 33% for most wavelengths. While the film material did not reach its minimum reflectivity at 850 nm as intended, the minimum reflectance was reached at a wavelength of approximately 880 nm. At 850 nm, the reflectivity was approximately 17%; at 880 nm, the reflectivity was as low as approximately 7%. At both wavelengths, the films served to significantly impact the reflectivity of the samples. Additionally, while the minimum reflectivity of the sample was not achieved at the intended 850 nm wavelength, only a very small change in the thickness of the films would be required to achieve the minimum reflectivity at the desired wavelength.

Conclusions

To develop additive manufacturing methods suitable for optical systems, this work has aimed to identify materials and processes to fabricate anti-reflective films. By varying the ink composition and printing parameters, control over film thickness with high resolution was investigated. With precise control of film thickness, the overall performance of AR films and spectral characteristics can be tailored, with possibilities for more complex designs providing broadband AR functionality. The ability to pattern such films with versatile, additive printing methods and high spatial resolution offers numerous advantages for advanced manufacturing of optical systems. Materials and methods from this work are readily adaptable and provide insight for implementation in additively manufactured fiber-optics.

Acknowledgements

References

1. Wu, L.; Dong, Z.; Li, F.; Zhou, H.; Song, Y., Emerging Progress of Inkjet Technology in Printing Optical Materials. *Advanced Optical Materials* **2016,** *4*, 1915-1932.
2. Moayedfar, M.; Assadi, M. K., Various Types of Anti-Reflective Coatings (ARCs) Based on the Layer Composition and Surface Topography: A Review. *Reviews on Advanced Materials Science* **2018,** *53*, 187-205.
3. Hedayati, M. K.; Elbahri, M., Antireflective Coatings: Conventional Stacking Layers and Ultrathin Plasmonic Metasurfaces, A Mini-Review. *Materials (Basel)* **2016,** *9*.
4. Johnson, R. W.; Hultqvist, A.; Bent, S. F. A brief review of atomic layer deposition: from fundamentals to applications. *Materials Today* **2014,** Volume 17, Issue 5, 236-246.

5. Pilvi, T.; Puukilainen, E.; Kreissig, U.; Leskelä, M.; Ritala, M. Atomic Layer Deposition of MgF$_2$ Thin Films Using TaF$_5$ as a Novel Fluorine Source. *Chemistry of Materials* **2008**, 20 (15), 5023-5028

6. Essien, M. Apparatuses and Methods for Stable Aerosol Deposition Using an Aerodynamic Lens System. US Appl. 14/927380, 2016.